ARTICLE

Properties of Eco-Friendly Oriented Strand Board Produced from Oil Palm Trunk

Ragil Widyorini[1,*], Greitta Kusuma Dewi[1], Arif Nuryawan[2], Eddy Heraldy[3] and Nanang Masruchin[4]

[1]Departement of Forest Product Technology, Faculty of Forestry, Universitas Gadjah Mada, Bulaksumur, Yogyakarta, 55281, Indonesia

[2]Departement of Forest Product Technology, Faculty of Forestry, Universitas Sumatra Utara, Medan, North Sumatra, 20155, Indonesia

[3]Department of Chemistry, Faculty of Mathematics and Natural Sciences, University of Sebelas Maret, Surakarta, Central Java, 57126, Indonesia

[4]Research Center for Biomass and Bioproducts, National Research and Innovation Agency (BRIN), Cibinong, West Java, 16911, Indonesia

[*]Corresponding Author: Ragil Widyorini. Email: rwidyorini@ugm.ac.id

ABSTRACT

Despite its considerable potential, oil palm trunk (OPT) remains underutilized, largely owing to the cyclical replanting process that occurs every 25–30 years. This study aimed to address this issue by developing an eco-friendly oriented strand board (OSB) using vascular bundles (VBs) from oil palm, both in binderless form and with the incorporation of natural adhesives made from sucrose and ammonium dihydrogen phosphate (ADP). The VB was extracted from OPT using a pressure cooker and mixed with a sucrose-ADP solution at various ratios. The mixture was then pressed at temperatures of 180°C and 200°C for 10 min to form boards, which were evaluated based on the Japanese Industrial Standard (JIS) A 5908 for particleboards. Binderless OSB was also manufactured without the use of any adhesive components. Fourier-transform infrared (FTIR) spectroscopy was conducted to evaluate the VB and its board. The results indicated that the mechanical properties of the binderless OSB met the JIS A 5908 Type 8 requirements. Furthermore, the addition of sucrose-ADP improved the physical and mechanical properties of the board, with an optimal sucrose-to-ADP ratio of 85:15. The OSB with the best properties met the JIS A 5908 Type 13 requirements. The FTIR results indicated that carbonyl groups, furan rings, and lignin played important roles in the bonding properties of the OSB. In conclusion, this research demonstrated the potential of VBs as a raw material for producing environmentally friendly OSB, both in binderless form and with the use of sucrose-ADP.

KEYWORDS

Oil palm trunk; vascular bundles; binderless OSB; sucrose; ammonium dihydrogen phosphate

1 Introduction

The rapid expansion of oil palm plantations is a significant phenomenon in Southeast Asia, particularly in Indonesia and Malaysia. Indonesia, in particular, is a major cultivator, with a total plantation area of approximately 14.59 million hectares reported in 2020 [1]. The peak yield of fresh fruit bunches occurs

between the 6th and 12th years after planting, after which it begins to decline. Replanting within a 25-year period has been observed to be optimal [2,3]. A substantial amount of biomass is generated from oil palm cultivation, especially during pruning and replanting. This biomass includes mesocarp fibers, fruit bunches, mill effluents, palm kernel shells, fronds, leaves, and trunks [4].

The potency of oil palm trunks (OPT) is particularly evident during the replanting season. According to Loh [5], the annual yield of OPT is approximately 3.6 million tons, which equates to 74.48 dry tons per hectare. Typically, the trunk is either burned or shredded and left on the plantation site for nutrient recycling [6]. However, prevalent burning practices present environmental challenges, which indicate that the utilization of OPT waste has not been fully optimized.

OPT has an anatomical structure that is mainly composed of fibers, tracheids, vessels, and ray parenchyma cells [4]. OPT has several disadvantages, including low strength, durability, dimensional stability, and machining characteristics [7]. Compared with wood, OPT is more porous, cellular, and anisotropic. Additionally, the high-density gradient along the longitudinal and radial axes makes it unsuitable for use as lumber without pretreatment [4,8]. However, OPT can be used in various wood-based products, such as pulp and paper [9,10], composite panels, plywood [11], laminated veneer lumber [12], glue-laminated timber [13], cross-laminated timber [14], particleboard [15], cement board [16], fiberboard [17], and acoustic materials [18]. Previous research has indicated that OPT fibers have acceptable strength for pulp and paper production, and composite panels show promising properties.

Hashim et al. [19,20] investigated the impact of particle geometry and temperature on OPT binderless particleboard. Their findings indicated that increased temperature enhanced the properties of the board. Additionally, OPT is characterized by high contents of holocellulose, lignin, starch, and sugars [20,21], which are crucial for self-bonding adhesion [22]. According to Ramle et al. [23], OPT can be separated into parenchyma and vascular bundles (VBs), with the VB categorized as strands based on their dimensions. The parenchyma is rich in sugars, starch, and saccharides. The separation process is driven by the non-durability of the palm stem. Nuryawan et al. [24] reported that OPT produces VB with an average length of 10.55 cm and a diameter of 0.67 mm. These dimensions align with recent research on oriented strand boards (OSBs) [25], despite differences in morphology, such as flat strands *vs*. cylindrical vascular bundles. OSB is defined as an engineered wood-based panel composed of strand elements (larger than chips) bonded and pressed together in layers [26,27]. OSBs play a crucial role in the construction industry and comprise approximately 66% of the structural panel market. Global production increased by more than 17% from 2020 to 2022 (from 38.5 to 45.1 million m^3) and is expected to remain consistent [27,28,29]. The manufacturing process involves synthetic adhesives, which present health and environmental concerns, such as formaldehyde-based and isocyanate-based adhesives. This has led to efforts to produce environmentally friendly OSBs using natural adhesives or non-formaldehyde materials.

According to Dirkes et al. [30], the major free sugars in OPT are sucrose and glucose, with sugar content ranging from approximately 16.97 to 140 mg/mL. In contrast, fresh VB yielded about 7–9 mg/mL of sugar when mechanically extracted from both longitudinal and radial directions [31]. Lamaming et al. [21] found that adding sucrose to binderless particleboard made from OPT enhances both strength and dimensional stability. In this context, sucrose functions as a natural binder for wood [32] and has been identified as a binderless board in previous research [21,33]. Moreover, the effectiveness of sucrose adhesives is significantly influenced by temperature [34]. Umemura et al. [34] reported that sucrose can be converted into a highly water-resistant substance with the addition of ammonium dihydrogen phosphate (ADP). Additionally, Zhao et al. [35,36] and Sun et al. [37] investigated sucrose-ADP adhesives, which are characterized by high solid content and suitable viscosity for plywood production. Zhao et al. [38] found that the optimal recycled wood particleboard was produced via the addition of 15% ADP to a sucrose-based adhesive.

Komariah et al. [39] explored the potential for bonding between ADP and water-soluble components within the inner part of OPT. They found that adding 10% ADP during particleboard manufacturing altered the properties by converting water-soluble components into insoluble components [39]. Additionally, the incorporation of sucrose had a significant impact, which highlights its relationship with the saccharide component [15]. This research aimed to investigate the physical and mechanical properties of OSBs, both with and without the addition of sucrose-ADP adhesives. The study included varying temperatures and examined the infrared spectra of the VB and the OSB.

2 Materials and Methods

2.1 Materials

VB were extracted from a 25-year-old OPT sourced from PT. Sawit Sumber Mas Sarana, Central Kalimantan, Indonesia. The bundles were obtained through a steam explosion process using a pressure cooker. After extraction, the VB was air-dried until the moisture content (MC) reached approximately 15% before being used as raw material. Fig. 1 shows the longitudinal and cross sections of the VB. The adhesive and catalyst solution comprised sucrose (Multi Kimia Raya Nusantara Co. Ltd., Semarang, Indonesia) and ADP (Merck, Darmstadt, Germany), with no additional treatment or purification.

Figure 1: Oil palm trunk vascular bundles, (A) longitudinal section and (B) cross-section

2.2 Preparation of Adhesive Solution

Within this framework, the solution was prepared by dissolving sucrose and ADP in distilled water to achieve a concentration of 50 wt%. The sucrose-to-ADP ratios in the solution were set at 95:5, 90:10, and 85:15 wt%. Additionally, an ADP solution was prepared by dissolving ADP in distilled water to a concentration of 30 wt%. Both solutions were prepared to achieve a 10 wt% content based on the air-dried weight of the strands.

2.3 Characterization of OPT VB

Considering this perspective, the length and diameter of OPT VB were characterized. The diameter was measured at the cross section of the VB using Dino Capture 2.0 software. For this analysis, cross-sectional images were obtained with a Digital Microscope (AM413ZT, Taiwan). In each cross section, five diameter measurements were taken at 36° intervals between two lines [40]. The average of these measurements was then calculated to determine the VB diameter.

2.4 Thermal Analysis of OPT VB

Thermal properties were characterized using a thermogravimetric analyzer (Leco TGA801, St. Joseph, MI, USA). The analysis was performed on raw OPT VB, VB sprayed with ADP solution, and VB treated with a 90:10 wt% sucrose-ADP solution, all at a 10 wt% content based on the air-dried weight of the

strands. The sprayed OPT VB were oven-dried at 80°C for 4 h [41] and then pulverized and screened to a size of less than 60 mesh. The prepared samples were heated at a rate of 25°C per minute, starting from room temperature (approximately 27°C) and increasing to 500°C under nitrogen purging.

2.5 Manufacture of OSBs

OSBs measuring 25 cm × 25 cm × 1 cm, with a target density of 0.75 g/cm^3, were manufactured with varying adhesive contents, sucrose-to-ADP ratios, and temperatures, as shown in Table 1. The binderless OSB, with 0 wt% adhesive content, was created by hot pressing three layers of OPT VB, with the strands oriented perpendicularly (90°) between layers. A single hot pressing session was conducted for 10 min at 3 MPa. Other three layer OSBs were made by spraying ADP or sucrose solutions onto the surface of the OPT VB, which were then oven-dried at 80°C for 4 h before hot pressing. The hot-pressing process was performed for 10 min via a three-step method [41], with all treatments performed in triplicate.

Table 1: Manufacturing condition of oriented strand boards

Adhesive content (wt%)	Sucrose-ADP ratio (wt%)	Concentration in solution (wt%)	Pressing temperature (°C)
0	–	–	180
0	–	–	200
10	0:100	30	180
10	0:100	30	200
10	95:5	50	180
10	90:10	50	180
10	85:15	50	180

2.6 Evaluation of OSBs

Before sample preparation and property evaluation, the OSB was conditioned at approximately 27°C and 77% relative humidity for one week. Following the Japanese Industrial Standard (JIS) A 5908 [42] guidelines, a comprehensive assessment of physical and mechanical properties was conducted. The physical properties evaluated included density, MC, thickness swelling (TS), water absorption (WA), and surface roughness (Ra). Mechanical properties evaluated were internal bonding (IB) strength, modulus of rupture (MOR), and modulus of elasticity (MOE). Samples measuring 5 cm × 5 cm × 1 cm were tested for density, MC, TS, WA, and IB strength, while bending strength and Ra were assessed for samples measuring 20 cm × 5 cm × 1 cm. For the TS and WA tests, samples were immersed in water at ambient temperature for 24 h, and changes were calculated as a percentage based on the initial values. The IB test was performed by applying vertical tension to the board surface at a rate of 2 mm/min until failure occurred. The static three-point bending test was conducted by applying a load perpendicular to the board surface at a speed of 10 mm/min and with a 15 cm span. Both the IB and bending tests were performed using a universal testing machine (Model 2260, Instron, Norwood, MA, USA), while Ra was measured using a Ra tester (SRG 400, Bosworth Instrument, Cleveland, OH, USA) at six random spots on both OSB surfaces. Each test was conducted in triplicate, and results are presented as average values with standard deviations.

2.7 Fourier-Transform Infrared Analysis

Fourier-transform infrared (FTIR) analysis was performed via the potassium bromide (KBr) disk method on both OPT VB raw materials and all OSB samples. The OSB samples were boiled for 2 h and then

immersed in water at ambient temperature for 1 h to remove any unreacted ADP and sucrose-ADP adhesive. The resulting mixture was ground into a powder. The OPT VB raw material was also ground directly into a powder without pretreatment. Samples with a particle size of less than 100 mesh were oven-dried at 60°C for 15 h. These samples were then scanned using an FTIR spectrophotometer (IR Prestige-21, Shimadzu, Kyoto, Japan) with 10 scans at a resolution of 16 cm^{-1} over a wavenumber range of 400–4000 cm^{-1}.

3 Result and Discussions

3.1 OPT VB Characterization

The longitudinal and cross sections of the OPT VB vessels and fiber components are shown in Fig. 1A,B. The observed lengths ranged from approximately 7 to 21 cm, and the diameters ranged from 0.69 to 1.33 mm. According to these dimensions, the OPT VB was classified as a strand. According to Irle et al. [43], a wood strand is defined as any material with length, thickness, and width dimensions within the ranges of 75–150 mm, 0.3–0.7 mm, and 15–25 mm, respectively. Additionally, wood strands measuring approximately 300 mm in length, 0.8 mm in thickness, and 25 mm in width are used to laminate boards and are marketed under the name TimberStrand® [44]. Considering this perspective, Parthasarathy et al. [45] reported that the diameter of palm VB ranges from 1–3 mm, depending on the stem location and species. This diameter is similar to that of date palm midribs, which are approximately 1 mm [46], but larger than the fibro-VB of *Salacca* fronds [47]. Larger fibro-VB diameters are often associated with lower mechanical properties, such as tensile strength and Young's modulus of the fibro-VB [47,48]. These factors may influence the properties of the composite board.

3.2 Thermal Analysis of OPT VB

The thermal analysis of OPT VB is shown in Fig. 2, with the highest weight reduction occurring between 255°C and 375°C. According to Komariah et al. [15,39], this temperature range exceeds the weight reduction temperatures observed in the inner part of OPT particles, which fall between 200°C and 350°C. The high α-cellulose content is identified as a possible reason for this difference. Additionally, the α-cellulose content in OPT VB is likely higher than that in parenchyma fibers, which are reportedly dominant in the inner part [49]. From this perspective, Wang et al. [50] and Yang et al. [51] noted that cellulose degradation in certain woods begins at temperatures above 320°C, while holocellulose experiences its greatest degradation at around 290°C.

The addition of 10 wt% ADP to OPT VB showed a tendency to preserve weight during thermal degradation. The weight was maintained at 38% at 400°C, whereas only 25% of OPT VB weight was sustained without ADP addition. OPT VB sprayed with sucrose-ADP at a 90:10 ratio exhibited thermal properties similar to the raw materials, although a slight weight loss was observed. Umemura et al. [34] noted that an increase in weight loss was also detected during the thermal analysis of sucrose combined with ADP.

3.3 Effect of ADP Addition and Pressing Temperature

Table 2 presents the MC, TS, WA, and Ra of OPT OSB, with varying proportions of ADP and different pressing temperatures. In this study, the MC of the boards ranged from 9.27%–12.14%, meeting the JIS A 5908 [42] standard requirement of 5%–13%. The binderless OSB pressed at 180°C exhibited high TS and WA values of 79% and 103%, respectively, which indicates relatively low dimensional stability and water resistance. However, a decrease of 72% and 25% in these parameters was observed when the pressing temperature was increased from 180°C to 200°C, thus indicating improved dimensional stability. Hashim et al. [20] and Lamaming et al. [21] reported that the TS value at 180°C was twice as high as that of OPT particleboard under similar conditions and a 20-min pressing duration. This suggests that extending the pressing time at a lower temperature of 180°C effectively reduces TS values. Additionally, the TS

values for binderless boards pressed at 200°C were consistent with previous studies conducted at the same temperature [20]. This research found that the TS values did not meet the JIS A 5908 standard requirement (maximum 12%). The high porosity of OPT VB, owing to the lumen of the vessels and fibers, contributed to the swelling of binderless OSB. Additionally, OPT VB was observed to contain free sugars, such as sucrose and glucose, as well as starch [31]. Sucrose-based particleboard was not water-resistant, and recycled wood boards manufactured with 20 wt% sucrose content at 180°C for 10 min were decomposed during the TS test [38].
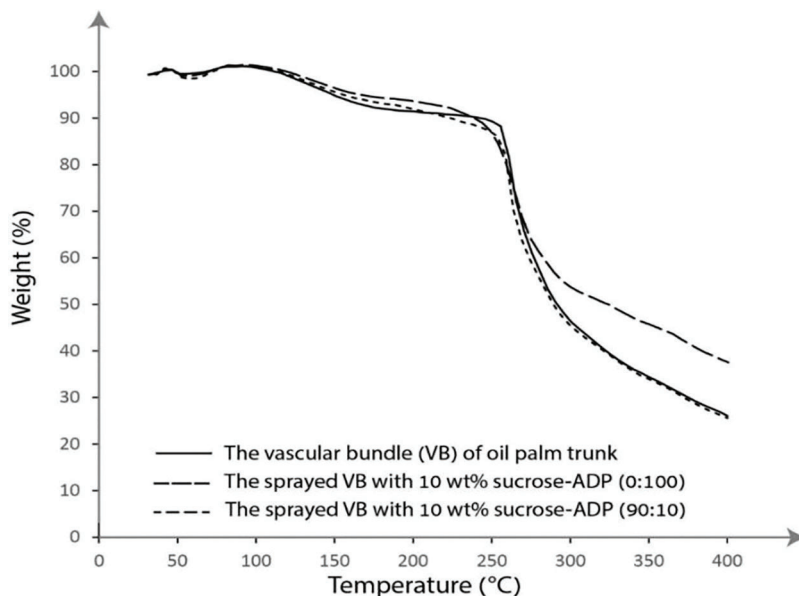
Figure 2: Thermogravimetric analysis of oil palm trunk vascular bundle and sprayed oil palm trunk vascular bundle

Table 2: MC, TS, WA, and Ra of binderless oriented strand boards

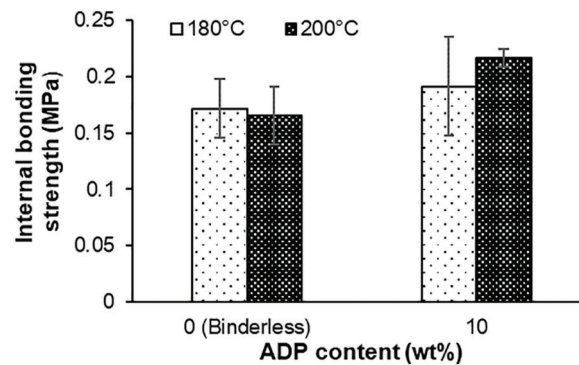| ADP content (wt%)	Pressing temperature (°C)	MC (%)	TS (%)	WA (%)	Ra (µm)
0	180	12.14 (0.41)	79.05 (4.37)	113.08 (5.78)	11.08 (1.49)
0	200	10.22 (1.65)	21.98 (1.87)	84.83 (20.72)	10.85 (3.60)
10	180	10.01 (1.03)	18.29 (2.42)	60.26 (13.20)	11.39 (4.54)
10	200	9.27 (1.46)	4.07 (0.62)	36.47 (3.10)	6.38 (1.12)

Note: Values in parentheses are standard deviations (n = 3).

According to these findings, the TS values met the JIS standard (maximum 12%) owing to the addition of 10% ADP at a pressing temperature of 200°C. The WA value for the OSB with 10% ADP also fell within the acceptable range of 20%–75% for particleboard [52]. These findings are consistent with those obtained in various studies on binderless particleboard made from OPT [39], sucrose-based particleboard [38,41], and plywood [35]. The presence of sugar-based substances and adhesives, combined with the addition of ADP and heat treatment, enhanced the water resistance of the raw material [39].

Ra values of OSBs were observed to be smoother with increased temperature and ADP addition. All values obtained were higher than the Ra of commercial particleboard in Japan, which ranges from 3.67–5.46 µm [53]. This discrepancy is attributed to the inherently rougher surface of VB compared with the

smaller particles typically used in commercial particleboard surface layers. However, the Ra of 6.36 ± 1.12 μm, achieved with 10% ADP addition and pressing at 200°C, was smoother than the commercial particleboard, which has a Ra range of 7.27 to 7.58 μm with isocyanate bonding [54,55].

The mechanical properties, including IB strength, MOR, and MOE, at varying ADP additions and pressing temperatures are shown in Figs. 3 and 4. The results indicate that binderless OSB can be manufactured from OPT VB through hot pressing without the need for additional adhesives. This effectiveness is attributed to chemical components such as sugars and starch, which act as bulking agents and play a significant role in the self-bonding process of the particles [22,56].

Figure 3: Internal bonding strength of oriented strand boards at different ADP contents and pressing temperatures. Vertical lines through the bars represent the standard deviation
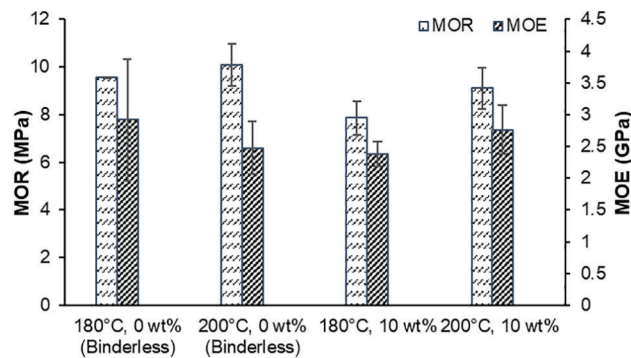
Figure 4: Modulus of rupture and modulus of elasticity of oriented strand boards at different ADP contents and pressing temperatures. Vertical lines through the bars represent the standard deviation

The addition of ADP improved the mechanical properties of OSBs. However, increasing the pressing temperature had only a minor effect on the internal bonding strength of the OSB. The IB values of the binderless boards ranged from 0.16–0.22 MPa, meeting the JIS A 5908 standard requirements. Binderless boards made from the inner part of OPT exhibited slightly higher IB values, which are attributable to the higher hemicellulose content in the inner OPT that enhances the self-bonding mechanism. The addition of 10 wt% ADP also improved the IB of the board, consistent with findings from previous research [39].

The MOR and MOE for the binderless OSB were 9.55 MPa and 2.92 GPa, respectively, meeting the JIS A 5908 standard requirements. These values were higher compared with those of binderless boards made from the inner part of OPT [39,56], which were tested at the same pressing temperature but for a longer duration of 20 min. The distinct geometry of the VB contributed remarkably to the higher MOR

compared with the inner part of the OPT. Additionally, the bending properties of the board improved with increasing pressing temperature. These findings indicate that the properties of the binderless board are influenced by the chemical composition of the raw materials, the particle geometry, and the processing conditions.

3.4 Effect of Sucrose-to-ADP Ratio

Table 3 presents the MC, Ra, TS, and WA of OSB produced from OPT VB using various sucrose-ADP adhesive ratios. The TS values ranged from 18.96%–9.77%. The addition of ADP reduced both TS and WA, which indicates improved dimensional stability and water resistance. Notably, all WA values were below 75%, meeting Food and Agriculture Organization (FAO) standards. The lowest TS and WA values were observed with a sucrose-to-ADP ratio of 85:15 wt%. The addition of sucrose significantly enhanced the physical properties and bonding mechanism when combined with ADP and OPT VB.

Table 3: MC, TS, WA, and Ra oriented strand boards made with sucrose-ADP adhesives

Sucrose-ADP ratio (wt%)	MC (%)	TS (%)	WA (%)	Ra (μm)
0:100	10.01 (1.03)	18.29 (2.42)	60.26 (13.20)	11.39 (4.54)
95:5	8.08 (0.98)	18.96 (2.51)	59.56 (22.28)	9.72 (4.03)
90:10	8.31 (1.56)	15.99 (3.75)	62.38 (18.82)	9.85 (2.40)
85:15	8.17 (2.16)	9.77 (3.02)	49.55 (1.79)	8.33 (2.47)

Note: Values in parentheses indicate the standard deviation (n = 3).

The Ra of the board decreased with increasing ADP content in the adhesives, resulting in a smoother surface. This improvement was attributed to the more compact contact between the VB fibers and the enhanced smoothness observed after hot-pressing. However, as shown in Table 2, the pressing temperature had a more significant impact on Ra than the sucrose-to-ADP ratios.

Fig. 5 shows the IB strength values of OSBs with varying sucrose-to-ADP ratios. The addition of sucrose-ADP (90:10) increased the IB by 78% and 88% compared with the addition of sucrose-ADP (95:5) and sucrose-ADP (0:100), respectively. This ratio achieved an IB value approximately twice as high as that of binderless particleboard. The IB value for sucrose-ADP (85:15) was comparable to that of sucrose-ADP (90:10). OSBs with sucrose-to-ADP ratios of 90:10 wt% and 85:15 wt% and subjected to a pressing temperature of 180°C met the Type 18 standard (minimum IB of 0.3 MPa). Additionally, the static bending strength values, including MOR and MOE shown in Fig. 6, generally met the Type 8 standards. An exception was observed with OSB containing a sucrose-to-ADP ratio of 0:100 wt% at 180°C. Similar trends were noted in the MOR and MOE, where increases of approximately 88% and 30%, respectively, were achieved compared with binderless treatments and sucrose-ADP (90:10). Moreover, sucrose-ADP (85:15) exhibited lower MOR and MOE than sucrose-ADP (90:10). OSB with sucrose-to-ADP ratios of 90:10 wt% and 85:15 wt% exhibited the highest mechanical properties, meeting the JIS A 5908 Type 13 standards for both MOR and MOE. According to Komariah et al. [15], a similar trend was observed in particleboards made from OPT. This suggests that variations in VB extraction and geometry did not significantly impact the mechanical properties of composite boards made from OPT and sucrose-ADP. According to this analysis, the most effective treatment was achieved with a sucrose-to-ADP ratio of 90:10 and a pressing temperature of 180°C.

The FTIR analysis of VB and OSB is shown in Fig. 7. The graph illustrates changes in intensity at wavelengths of 1705, 1620, 1512, 1249, 895, and 771 cm^{-1}, indicating potential modifications in the compounds. These changes are attributed to the hydrolysis of chemical components from VB and sucrose. Absorption in the region between 1700 and 1800 cm^{-1} corresponded to the stretching vibrations

of the carbonyl (C=O) functional group [57,58]. The peak at 1705 cm^{-1} increased with rising pressing temperatures owing to the deacetylation process. Peaks between 1600 and 1638 cm^{-1} represented absorbed water, β-glucosidic linkages between sugar units, and hemicellulose degradation [58]. The binderless board exhibited the strongest peak at 1620 cm^{-1}, attributed to hemicellulose, a key component in the manufacturing process [22].
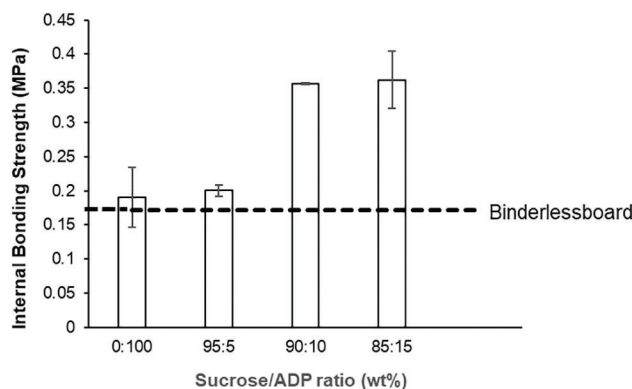

Figure 5: Internal bonding strength of oriented strand boards at various sucrose-to-ADP ratios. Vertical lines through the bars indicate the standard deviation
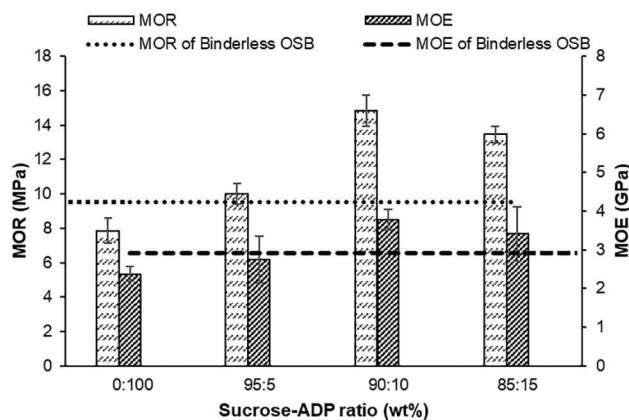
Figure 6: Modulus of rupture and modulus of elasticity of oriented strand boards at different sucrose-to-ADP ratios. Vertical lines through the bars indicate the standard deviation

The peak at 1512 cm^{-1} corresponded to the C=C aromatic ring vibrations in lignin [59] and the presence of furan in sucrose heated with ADP [37]. In the infrared spectra of OPT VB and OSB (Fig. 7), the peak at 1512 cm^{-1} in OPT VB showed lower intensity compared with that in the binderless, ADP, and sucrose-ADP bonded boards. This suggests that the furan ring significantly contributed to the bonding process and enhanced the physical and mechanical properties of the board. According to Cheng et al. [60] and Lee et al. [58], the peak at 1249 cm^{-1} corresponded to syringyl ring breathing and C-O stretching in lignin and xylan. The intensity of this peak decreased in OPT VB after heat treatment, which indicates the degradation of lignin and hemicellulose. Additionally, the peak at 895 cm^{-1}, attributed to the depolymerization of hemicellulose [58,61], found in OPT VB and binderless boards, while other samples exhibited a reduction in this peak.
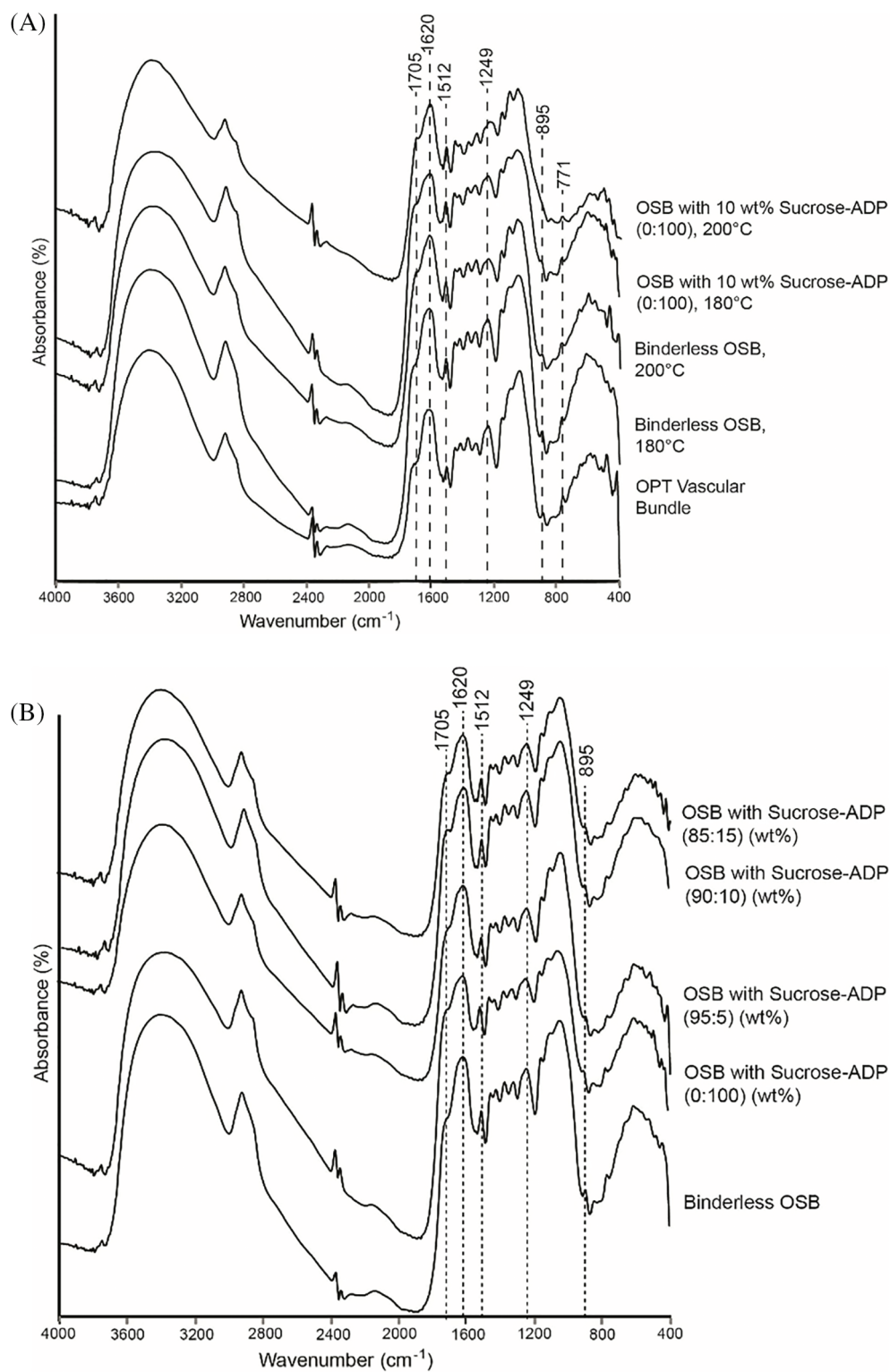
Figure 7: Infrared spectra of oil palm trunk vascular bundle and oriented strand board, (A) Effect of ADP addition and pressing temperature and (B) Effect of sucrose-to-ADP ratios at a pressing temperature of 180°C

4 Conclusion

In conclusion, VB derived from OPT was effectively used as raw material for producing OSBs, both as a binderless board and with the addition of a sucrose-ADP adhesive. The results indicated that binderless OSB met the JIS A 5908 Type 8 standard for mechanical properties. However, the addition of sucrose-ADP significantly enhanced these properties. Notably, while ADP alone did not improve mechanical properties, the inclusion of sucrose-ADP allowed the board to meet the JIS A 5908 Type 13 standard requirements. This demonstrates that VB from OPT is a viable, renewable resource for producing biocomposite products.

Author Contributions: The authors confirm contribution to the paper as follows: study conception and design: Ragil Widyorini, Greitta Kusuma Dewi, Arif Nuryawan, Eddy Heraldy, Nanang Masruchin; data collection: Ragil Widyorini, Greitta Kusuma Dewi, Arif Nuryawan; analysis and interpretation of results: Ragil Widyorini, Greitta Kusuma Dewi; draft manuscript preparation: Ragil Widyorini, Greitta Kusuma Dewi. All authors reviewed the results and approved the final version of the manuscript.

Availability of Data and Materials: The data is accessible on request to the authors.

Ethics Approval: Not applicable.

Conflicts of Interest: The authors declare that they have no conflicts of interest to report regarding the present study.

References

1. Directorate of Livestock, Fisheries, and Forestry Statistics. Statistics of forestry production 2021. Jakarta: BPS-Statistics Indonesia; 2021.

2. Zhao J, Elmore AJ, Lee JSH, Numata I, Zhang X, Cochrane MA. Replanting and yield increase strategies for alleviating the potential decline in palm oil production in Indonesia. Agric Syst. 2023;210:103714. doi:10.1016/j.agsy.2023.103714.

3. Pulingam T, Lakshmanan M, Chuah J-A, Surendran A, Zainab-L I, Foroozandeh P, et al. Oil palm trunk waste: environmental impacts and management strategies. Ind Crops Prod. 2022;189:115827. doi:10.1016/j.indcrop.2022.115827.

4. Nuryawan A, Sutiawan J, Rahmawaty, Masruchin N, Bekhta P. Panel products made of oil palm trunk: a review of potency, environmental aspect, and comparison with wood-based composites. Polymers. 2022;14(9):1758. doi:10.3390/polym14091758.

5. Loh SK. The potential of the Malaysian oil palm biomass as a renewable energy source. Energy Convers Manag. 2017;141(658):285–98. doi:10.1016/j.enconman.2016.08.081.

6. Nudri NA, Bachmann RT, Ghani WAWAK, Sum DNK, Azni AA. Characterization of oil palm trunk biocoal and its suitability for solid fuel applications. Biomass Convers Biorefin. 2020;10(1):45–55. doi:10.1007/s13399-019-00419-z.

7. Myśkow E, Błaś M, Sobik M, Godek M, Owczarek P. The effect of pollutant fog deposition on the wood anatomy of subalpine Norway spruce. Eur J Forest Res. 2019;138(2):187–201. doi:10.1007/s10342-018-01160-4.

8. Srivaro S, Matan N, Lam F. Property gradients in oil palm trunk (*Elaeis guineensis*). J Wood Sci. 2018;64(6):709–19. doi:10.1007/s10086-018-1750-8.

9. Low LQ, Ilyas RA, Jalil R, Hawanis HSN, Ibrahim R, Azriena HAA, et al. Physical and mechanical enhancement of beaten oil palm trunk pulp and paper by optimizing starch addition: towards sustainable packaging solutions. Ind Crops Prod. 2024;221:119232. doi:10.1016/j.indcrop.2024.119232.

10. Onuorah EO, Nwabanne JT, Nnabuife ELC. Pulp and paper making potentials of *Elaeis guineensis* (oil palm) grown in southeast. Nigeria World J Eng. 2015;12(1):1–12. doi:10.1260/1708-5284.12.1.1.

11. Ismail AC, Salim S, Tahir PM, Lee SH, Ghani MA, Edrus SSA, et al. Properties enhancement of oil palm trunk plywood against decay and termite for marine applications. Polymers. 2022;14(3):2680. doi:10.3390/polym14132680.

12. Ghani A, Lee SH, Sabaruddin FA, SaifulAzry SOA, Paridah MT. Laminated veneer lumber from oil palm trunk. In: Sapuan SM, Paridah MT, SaifulAzry SOA, Lee SH, editors. Oil palm biomass for composite panels: fundamentals, processing, and applications. Amsterdam: Academic Press; 2022. p. 241–51.

13. Prabuningrum DS, Massijaya MY, Hadi YS, Abdillah IB. Physical-mechanical properties of laminated board made from oil palm trunk (*Elaeis guineensis* Jacq.) waste with various lamina compositions and densifications. J Korean Wood Sci Technol. 2020;48(2):196–205. doi:10.5658/wood.2020.48.2.196.

14. Srivaro S, Matan N, Lam F. Performance of cross laminated timber made of oil palm trunk waste for building construction: a pilot study. Eur J Wood Prod. 2019;77(3):353–65. doi:10.1007/s00107-019-01403-0.

15. Komariah RN, Krishanti NPRA, Yoshimura T, Umemura K. Characterization of particleboard using the inner part of oil palm trunk (OPT) with a bio-based adhesive of sicrose-ammonium dihydrogen phosphate (ADP). BioResources. 2022;17(3):5190–206. doi:10.15376/biores.17.3.5190-5206.

16. Sudarmanto, Juwono AL, Subyakto, Budiman I, Lubis MAR, Kusumah SS, et al. Effect of cold-water treatment and hydrothermal carbonization of oil-palm-trunk fibers on compatibility with cement for-bonded particleboard. Wood Mater Sci Eng. 2021;17(6):979–88. doi:10.1080/17480272.2021.1983871.

17. Awang R, Wahab NA, Ibrahim Z, Aziz AA. Medium density fiberboard (MDF) from oil palm fibre: a review. Malays J Anal Sci. 2023;27(3):626–40.

18. Manik TN, Nuki SA, Fauziyah NA, Mashuri, Zainuri M, Darminto. Structure, dynamic- mechanical and acoustic properties of oil palm trunk modified by melamine formaldehyde. J Renew Mater. 2021;9(9):1647–60. doi:10.32604/jrm.2021.016089.

19. Hashim R, Saari N, Sulaiman O, Sugimoto T, Hiziroglu S, Sato M, et al. Effect of particle geometry on the properties of binderless particleboard manufactured from oil palm trunk. Mater Des. 2010;31(9):4251–7. doi:10.1016/j.matdes.2010.04.012.

20. Hashim R, Said N, Lamaming J, Baskaran M, Sulaiman O, Sato M, et al. Influence of press temperature on the properties of binderless particleboard made from oil palm trunk. Mater Des. 2011;32(5):2520–5. doi:10.1016/j.matdes.2011.01.053.

21. Lamaming J, Hashim R, Sulaiman O, Sugimoto, Sato M, Hiziroglu S. Measurement of some properties of binderless particleboards made from young and old oil palm trunks. Measurement. 2014;47(2):813–9. doi:10.1016/j.measurement.2013.10.007.

22. Widyorini R, Higashihara T, Xu J, Watanabe T, Kawai S. Self bonding characteristics of binderless kenaf core composite. Wood Sci Technol. 2005;39(8):651–62. doi:10.1007/s00226-005-0030-0.

23. Ramle SFM, Sulaiman O, Hashim R, Arai T, Kosugi A, Abe H, et al. Characterization of parenchyma and vascular bundle of oil-palm as function of storage time. Lignocellulose. 2012;1(1):33–44.

24. Nuryawan A, Dalimunthe A, Saragih RN. Physical and chemical properties of oil palm trunk vascular bundles. FORESTA: Indones J For. 2012;1(2):34–40.

25. Lunguleasa A, Dumitrascu AE, Spirchez C, Ciobanu VD. Influence of the strand characteristics on the properties of oriented strand boards obtained from resinous and broad-leaved fast-growing species. Appl Sci. 2021;11(4):1784. doi:10.3390/app11041784.

26. Nishimura T. Chipboard, oriented strand board (OSB) and structural composite lumber. In: Ansell MP, editor. Wood composites. Sawston: Woodhead Publishing; 2015. p. 103–21.

27. Gong J, Zhu H, Zhou H, Stoliarov SI. Development of pyrolysis model for oriented strand board. Part I: kinetics and thermodynamics of the thermal decomposition. J Fire Sci. 2021;39(2):190–204. doi:10.1177/0734904120982887.

28. FAO. Forest production and trade. OSB production quantity in the world. 2023. Available from: http://www.fao.org/faostat/en/#data/FO. [Accessed 2024].

29. UNECE. UNECE/FAO forest products annual market review 2022–2023. Geneva: United Nations Publication; 2023.

30. Dirkes R, Neubauer PR, Rabenhorst J. Pressed sap from oil palm (*Elaeis guinensis*) trunks: a revolutionary growth medium for the biotechnological industry? Biofuel Bioprod Biorefin. 2021;15(3):931–44. doi:10.1002/bbb.2201.

31. Ramle SFM. Chemical composition of parenchyma and vascular bundle from *Elaeis guineensis*. In: Kamyab H, editor. Elaeis guineensis. London: IntechOpen; 2021. p. 98421.

32. Pizzi A, Papadopoulos AN, Policardi F. Wood composites and their polymer binders. Polymers. 2020;12(5):1115. doi:10.3390/polym12051115.

33. Nadhari WNAW, Ishak NS, Danish M, Atan S, Mustapha A, Karim NA, et al. Mechanical and physical properties of binderless particleboard made from oil palm empty fruit bunch (OPEFB) with addition of natural binder. Mater Today: Proc. 2020;31(1):287–91. doi:10.1016/j.matpr.2020.06.009.

34. Umemura K, Hayashi S, Tanaka S, Kanayama K. Changes in physical and chemical properties of sucrose by the addition of ammonium dihydrogen phosphate. J Adhes Soc Japan. 2017;53(4):112–7. doi:10.11618/adhesion.53.112.

35. Zhao Z, Sun S, Wu D, Zhang M, Huang C, Umemura K, et al. Synthesis and characterization of sucrose and ammonium dihydrogen phosphate (SADF) adhesive for plywood. Polymers. 2019;11(12):1909. doi:10.3390/polym11121909.

36. Zhao Z, Sakai S, Wu D, Chen Z, Zhu N, Gui C, et al. Investigation of synthesis mechanism, optimal hot-pressing conditions, and curing behavior of sucrose and ammonium dihydrogen phosphate adhesive. Polymers. 2020;12(1):216. doi:10.3390/polym12010216.

37. Sun S, Zhang M, Umemur K, Zhao Z. Investigation and characterization of synthesis conditions on sucrose-ammonium dihydrogen phosphate (SADP) adhesive: bond performance and chemical transformation. Materials. 2019;12(24):4078. doi:10.3390/ma12244078.

38. Zhao Z, Hayashi S, Xu W, Wu Z, Tanaka S, Sun S, et al. A novel eco-friendly wood adhesive composed by sucrose and ammonium dihydrogen phosphate. Polymers. 2018;10(11):1251. doi:10.3390/polym10111251.

39. Komariah RN, Miyamoto T, Tanaka S, Prasetiyo KW, Syamani FA, Subyakto, et al. High-performance binderless particleboard from the inner part of oil palm trunk by addition of ammonium dihydrogen phosphate. Ind Crop Prod. 2019;141(3):111761. doi:10.1016/j.indcrop.2019.111761.

40. Munawar S, Umemura K, Tanaka F, Kawai S. Characterization of the morphological, physical, and mechanical properties of seven nonwood plant fiber bundles. J Wood Sci. 2007;54(2):28–35. doi:10.1007/s10086-006-0836-x.

41. Widyorini R. Evaluation of physical and mechanical properties of particleboard made from petung bamboo using sucrose-based adhesive. BioResources. 2020;15(3):5072–86. doi:10.15376/biores.15.3.5072-5086.

42. JIS A 5908. JIS for particleboard. Tokyo: Japanese Industrial Standard; 2003.

43. Irle M, Barbu MC. Wood-based panel technology. In: Thoeman H, Irle M, Sernek M, editors. Wood-based panels: an introduction for specialists. London: Brunel University Press; 2010. p. 1–90.

44. Meyers KL. Impact of strand geometry and orientation on mechanical properties of strand composites (Master Thesis). Washington State University: Washington, DC, USA; 2001.

45. Parthsarathy MV, Klotz LH. Palm "wood" I. Anatomical aspects. Wood Sci Technol. 1976;10(3):215–29. doi:10.1007/bf00355742.

46. Elseify LA, Midani M, Hassanin AH, Hamouda T, Khiari R. Long textile fibres from the midrib of date palm: physiochemical, morphological, and mechanical properties. Ind Crops Prod. 2020;151:112466. doi:10.1016/j.indcrop.2020.112466.

47. Hakim L, Widyorini R, Dwi Nugroho W, Prayitno TA. Anatomical, chemical, and mechanical porperties of fibrovascular bundels of salacca (snake fruit) frond. BioResources. 2019;14(4):7943–57. doi:10.15376/biores. 14.4.7943-7957.

48. Zhai S, Imai T, Horikawa Y, Sugiyama J. Anatomical and mechanical characteristics of leaf-sheath fibrovascular bundles in palms. IAWA J. 2013;34(3):285–300. doi:10.1163/22941932-00000024.

49. Ramle SFM, Othman S, Hashim R, Hamid ZAA, Arai T, Kosugi A, et al. Chemical characterization from parenchyma and vascular bundle at different parts of oil palm trunk. AIP Conf Proc. 2019;2068:020039. doi:10.1063/1.5089338.

50. Wang J, Minami E, Kawamoto H. Thermal reactivity of hemicellulose and cellulose in cedar and beech wood cell walls. J Wood Sci. 2020;66(1):41. doi:10.1186/s10086-020-01888-x.

51. Yang W, Fang M, Xu H, Wang H, Wu S, Zhou J, et al. Interactions between holocellulose and lignin during hydrolysis of sawdust in subcritical water. ACS Sustain Chem Eng. 2019;7(12):10583–94. doi:10.1021/acssuschemeng.9b01127.

52. Anosike-Francis EN, Obianyo II, Salami OW, Ihekweme GO, Ofem MI, Olorunnisola AO, et al. Physical-mechanical properties of wood based composite reinforced with recycled polypropylene and cowpea (*Vigna unguiculata* Walp.) husk. Cleaner Mater. 2022;5:100101. doi:10.1016/j.clema.2022.100101.

53. Hirizoglu S, Suzuki SV. Evaluation of surface roughness of commercially manufactured particleboard and medium density fiberboard in Japan. J Mater Process Tech. 2007;184:436–40. doi:10.1016/j.jmatprotec.2006.11.011.

54. Del Menezzi CHS, Ribeiro RB, Sternadt GH, Teixira DE, Okino EYA. Effect of thermal post-treatment on some surface-related properties of oriented strandboards. Drvna Ind. 2008;59(2):61–7.

55. Copak A, Jirouš-Rajković V, Španić N, Miklečić J. The impact of post-manufacture treatments on the surface characteristics important for finishing of OSB and particleboard. Forests. 2021;12(8):975. doi:10.3390/f12080975.

56. Lamaming J, Sulaiman O, Sugimoto T, Hashim R, Said N, Sato M. Influence of chemical components of oil palm on properties of binderless particleboard. BioResources. 2013;8(3):3358–71. doi:10.15376/biores.8.3.3358-3371.

57. Peng Q, Ormondroyd G, Spear M, Chang WS. The effect of the changes in chemical composition due to thermal treatment on the mechanical properties of *Pinus densiflora*. Constr Build Mater. 2022;358(3):129303. doi:10.1016/j.conbuildmat.2022.129303.

58. Lee SH, Ashaaria Z, Ang AF, Halipa JA, Lum WC, Dahali R, et al. Effects of two-step post heat-treatment in palm oil on the properties of oil palm trunk particleboard. Ind Crops Prod. 2018;116:249–58. doi:10.1016/j.indcrop.2018.02.050.

59. Yefremova S, Zharmenov A, Sukharnikov Y, Bunchuk L, Kablanbekov A, Anarbekov K, et al. Rice husk hydrolytic lignin transformation in carbonization process. Molecules. 2019;24(17):3075. doi:10.3390/molecules24173075.

60. Cheng XC, Cui XY, Qin Z, Liu HM, Wang XD, Liu YL. Effect of drying pretreatment methods on structural features and antioxidant activities of Brauns native lignin extracted from Chinese quince fruit. Process Biochem. 2021;106(3):70–7. doi:10.1016/j.procbio.2021.04.004.

61. Puițel AC, Suditu GD, Danu M, Ailiesei GL, Nechita MT. An experimental study on the hot alkali extraction of xylan-based hemicelluloses from wheat straw and corn stalks and optimization methods. Polym. 2022;14(9):1662. doi:10.3390/polym14091662.